The sampling volume of trawl and acoustics: estimating availability probabilities from observations of tracked individual fish

Nils Olav Handegard and Dag Tjøstheim

Abstract: The effective sampling volume of trawl and acoustics is an important parameter in fish abundance estimation surveys. This paper presents a method to compute the probability of a fish being available to the bottom trawl and the probability of it being seen on the echo sounder, given its initial position relative to the vessel path. These probabilities are then related to the calculation of the effective observational volume for trawl and acoustics, the two main tools of measuring abundance of Atlantic cod (*Gadus morhua*) and haddock (*Melanogrammus aeglefinus*). As an example, the computation is carried out for a typical vertical distribution in the Barents Sea. Our model is based on an Ornstein–Uhlenbeck model for the fish swimming trajectories, and its parameters are estimated using observations of swimming trajectories for individual fish, recorded by a split-beam echo sounder. The model itself constitutes a general method to translate observations on behaviour of individual fish to probability maps. The results indicate a typical fishing height of 20 m for the bottom trawl, but it is also shown that there is a relatively low probability of catching by the trawl what you see on the echo sounder, even for fish positioned directly in the trawl path. This is because of strong lateral movements of the fish.

Résumé : Le volume effectivement échantillonné est une variable importante dans les inventaires d'abondance des poissons faits par chalutage ou par acoustique. Notre travail présente une méthode pour calculer la probabilité qu'un poisson soit accessible au chalut de fond et qu'il soit visible sur l'échosondeur, étant donné sa position initiale relative à la trajectoire du navire. Ces probabilités peuvent ensuite être reliées au calcul du volume effectif obtenu par chalutage ou acoustique, les deux outils principaux pour mesurer l'abondance de la morue franche (*Gadus morhua*) et l'aiglefin (*Melanogrammus aeglefinus*). Le calcul d'une répartition verticale typique de la mer de Barents est donné en exemple. Notre modèle se base sur le modèle d'Ornstein–Uhlenbeck des trajectoires de nage des poissons et les paramètres sont estimés à partir d'observations de trajectoires de nage de poissons individuels enregistrées par un échosondeur à faisceau divisé. Le modèle lui-même représente une méthode générale pour traduire des observations faites sur un seul poisson individuel en cartes de probabilité. Nos résultats indiquent que la hauteur moyenne typique de pêche d'un chalut de fond est de 20 m, mais aussi qu'il y a une probabilité relativement faible de capture par le chalut des poissons visibles à l'échosondeur, même pour les poissons placés directement dans la trajectoire du chalut; cela s'explique par l'importance des déplacements latéraux des poissons.

[Traduit par la Rédaction]

Introduction

Two problems in fish survey methodology that have been subject to intense research are (*i*) absolute abundance estimation (Løland et al. 2007) and (*ii*) relating bottom trawl and acoustic estimates (Aglen 1996; Hjellvik et al. 2003, 2007). To arrive at an estimate of absolute abundance from trawl catches, the effective catching volume and the gear selection are needed. Moreover, to combine acoustics and trawl data, one has to take into account that these data come from two different parts of the water column, with no clear separation between the two.

Received 1 April 2008. Accepted 27 October 2008. Published on the NRC Research Press Web site at cjfas.nrc.ca on 10 March 2009.
J20486

N.O. Handegard.[1] Institute of Marine Research, P.O. Box 1870, Nordnes, 5817 Bergen, Norway.
D. Tjøstheim. Department of Mathematics, University of Bergen, P.O. Box 7800, 5020 Bergen, Norway.

[1]Corresponding author (e-mail: nilsolav@imr.no).

For both problems, understanding vessel-induced fish behaviour is essential. A fish may end up not being registered by the trawl or acoustics even though it was initially positioned where unchanged behaviour would lead to its capture or detection. On the other hand, there is a herding effect such that the bottom trawl may capture fish that were positioned above the trawl headline when the vessel passed and the acoustic estimates were recorded. That the vessel and (or) gear initiates a fish reaction has been acknowledged for a long time (Okonski 1969). It may start before the vessel arrives and is combined with a stronger response just after propeller passage (Ona and Godø 1990; Nunnallee 1991). De Robertis and Wilson (2006) reported significantly higher average backscatter from the vessel-mounted echo sounder when free-running than during trawling, indicating increased vessel avoidance during trawling, but opposite results were found by Hjellvik et al. (2007). Similar studies have been carried out for the acoustic estimate separately. Olsen et al. (1983) showed that fish reacted to an approaching surveying vessel. Vabø et al. (2002) reported a strong response in Atlantic herring (*Clupea harengus*), whereas Fernandes et al.

(2000*a*) reported no reaction. The latter was attributed to a silent vessel design (Fernandes et al. 2000*b*), but this has later been questioned (Ona et al. 2007).

The previous reports are based on measuring changes in fish density by a small boat or stationary transducer as the vessel passes. As opposed to those investigations, Handegard et al. (2003) and Handegard and Tjøstheim (2005) used observations from a free-floating buoy equipped with a split-beam echo sounder to track and analyze the behaviour of individual gadoid fish (mainly Atlantic cod (*Gadus morhua*), saithe (i.e., pollock, *Pollachius virens*), and haddock (*Melanogrammus aeglefinus*)), and they were able to describe the avoidance reactions in terms of average velocity changes, both vertically and horizontally. In the present study, we are more ambitious, and we are seeking to characterize distributional changes, i.e., take into account the variability in the response, not only the mean response.

Dickson (1993*a*) provided a framework for evaluating the capture efficiency of trawls, and the model was parameterized for the Barents Sea survey condition using various sources of data (Dickson 1993*b*). However, there were no data for estimating the parameters for the model before the arrival of the trawl doors. We believe that our results can be used to fill this gap.

Typical questions that can be asked about availability are as follows: What proportion of the fish outside the acoustic dead zone are available for the trawl? Given a fish located at a certain position relative to the course line of the approaching vessel, what is the probability of it being observed by the echo sounder? How far in the horizontal and vertical directions does the catching capability of the trawl extend? Is it easier to catch fish at a certain horizontal distance from the trawl than a fish at the same vertical distance from the trawl? Answers to these questions will have implications both for acoustic and trawl surveys. But we also think that these are problems of independent interest because the reaction pattern of the fish tells something about its sensing apparatus and associated behaviour.

We will use a modelling approach based on the Ornstein–Uhlenbeck (OU) diffusion process to attack the above problems, and we will use the same data as in Handegard and Tjøstheim (2005). Finally, we put our results in perspective by presenting them in terms of parameters for Dickson's model.

Materials and methods

The fish-capture process of the bottom trawl is a truly four-dimensional process, with three spatial and one temporal dimension. Traditionally, one-dimensional properties like fishing heights (Aglen 1996; Aglen et al. 1999; Hjellvik et al. 2003) and effective path widths (Engås and Godø 1989; Ramm and Xiao 1995) have been investigated. Effective path width is a measure of how far to the side of the centre of the trawl fish are caught, it being governed by sweeping and herding effects, trawl selection, etc. The fishing height determines how far up in the water column the trawl catches fish by downward herding. This results in a rectangular interpretation of the fishing volume, since path width combined with trawl height defines a rectangle.

In this paper, the process is treated in a three-dimensional setting: depth (z), athwartship direction (y), and time (t). Let $\boldsymbol{x}(t) = [y(t), z(t)]$ be a vector that describes the coordinates of a fish at time t in the y–z plane. The behaviour along the vessel path (x) is ignored because of the large difference in vessel speed and alongship fish velocity (cf. Discussion). The behaviour described by our model is thus the projection of three-dimensional swimming velocities onto a two-dimensional y–z plane perpendicular to the vessel path, where the y–z plane is fixed in space. The centre of the buoy echo beam lies in this plane, and the observations from this are used to estimate the parameters of the model. The vessel and gear pass this plane, where the change in behaviour measured in terms of velocity changes for individual fish can be observed (see Fig. 1). A List of symbols is given at the end of the paper.

Data and tracking method

This section presents a brief overview of the data and the tracking method. A detailed description of the experimental design, species composition, geographical area, and analysis of the data can be found in Handegard and Tjøstheim (2005).

A free-floating buoy containing a Simrad EK60 echo sounder was placed in the path of the vessel, and single fish were detected and tracked as the vessel and gear approached and passed the buoy. The data set consisted of 54 vessel–buoy passings, recorded during trawling using R/V *G.O. Sars* (built in 1970) over two time periods (March 2001 and April 2002). A brief overview of the observed behavioural pattern is given (Fig. 2).

A crucial part of the analysis is the tracking algorithm. We have used an algorithm designed for a moving platform (Handegard et al. 2005). A brief resumé of the tracking method is given in the following. Single fish targets are detected using the Simrad single echo detection algorithm, and the single echoes are combined into tracks. The transducer platform tilt–roll–heave is estimated from the common movement of the fish within the beam (Handegard et al. 2005, see their figure 5). Then a second run is performed to compensate for the estimated platform movement. The tracking parameters are set equal to "case 1" in Handegard et al. (2005, their table V).

After the single fish echoes have been associated to tracks, several algorithms can be used to estimate the fish trajectories. We have chosen more than one smoothing algorithm to get an estimate of the sensitivity to various alternatives. The algorithms we have used are Kalman smoothing, nonparametric splines with cross validation and parametric splines with four different levels of smoothing. These methods are described as the KS, SNP, and SP methods, respectively, in Handegard et al. (2005). The smoothing parameter "spar" for the parametric spline is set to 0.3, 0.5, 0.7, and 0.9, resulting in a total of six different algorithms or levels of smoothing (cf. Fig. 3). Although the estimated velocities may be biased (Handegard and Tjøstheim 2005, their section 4.1.), we assume here that they reflect true displacement velocities.

The buoy, vessel, and gear are positioned using the buoy's and vessel's global positioning system (GPS) and the Simrad ITI trawl positioning system (Engås et al. 2000) for the trawl. All pings in a track are positioned relative to

Fig. 1. Schematic overview of the model. The size of the rectangular y–z plane corresponds to the axes in Figs. 6, 7, and 9. The position of the trawl, warps, and vessel are shown. The x axis shows estimated distances computed from the time t before or after vessel passing assuming a constant vessel speed v: $x = vt$. The dots depict simulated (2D) individual fish, with the plus sign as the starting position. The objective of the paper is to develop and use this simulation model. To view the video, see the HTML Web version of this paper at cjfas.nrc.ca.

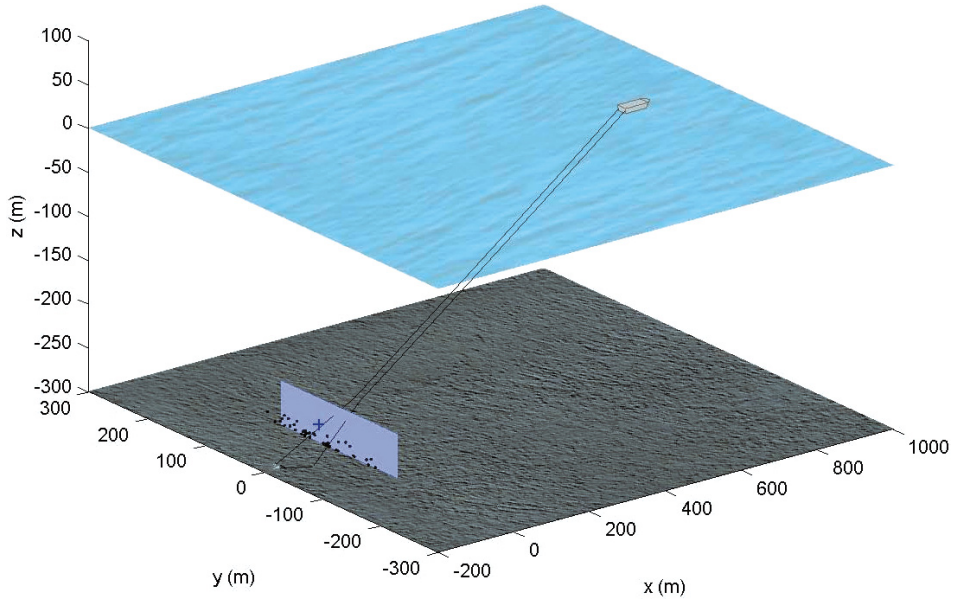

Fig. 2. A typical reaction pattern as reported in Handegard and Tjøstheim (2005). The background image is the echogram from the buoy at one buoy–vessel passing. Tracking individuals showed that the fish responded as early as 15 min before the vessel arrived, with increased diving (I). At vessel passing, there was a weak herding in front of the vessel combined with a stronger diving and herding towards the vessel track (II). The strongest response was observed as swimming away from the trawl warps, both by diving and horizontal avoidance (III). The diagonal line represents the position of the warps. Vertical lines above the trawl are noise from the trawl sensors. The cone represents the vessel-mounted echo sounder.

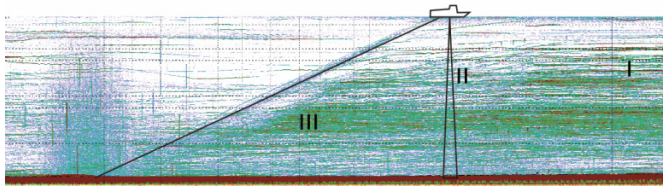

Fig. 3. Example of a track projected onto the y–z plane. The figure shows the same track with different smoothing estimators. The curve at the top is the smoothing spline estimator, SP, with spar equal to 0.3, followed by the SP with spar equal to 0.5, 0.7, and 0.9. The fifth curve is the smoothing spline with cross validataion, SNP, and the last curve is the Kalman smoothing estimator, KS. The curves are cumulatively shifted 1 m downwards to distinguish one from the other.

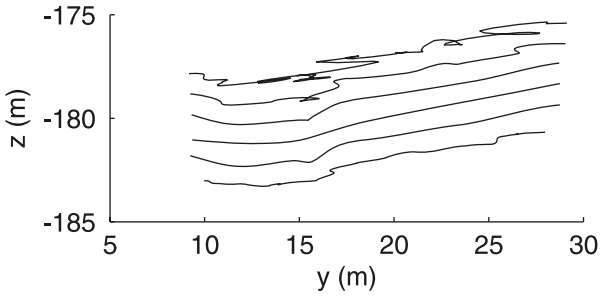

the vessel using the athwartship position (y) and vertical position (z). The projection of a track onto the y–z plane results in a curve, such as in Fig. 3. Each position in a track is also associated with a time t measured on a time scale whose origin is the time when the vessel passes the buoy. Time points before vessel passage are negative on the time scale. The fish behaviour is assumed to be symmetric around the alongship direction of the vessel, i.e., the athwartship position y is multiplied with sign(y), where "sign" is the signum function, which equals 1 if y is positive and –1 if negative. Note that we use the raw data, not the data corrected for water currents as in Handegard and Tjøstheim (2005). The reason is that in the previous work we wanted to detect changes in behaviour, whereas here we would like to estimate how a fish moves relative to the trawl path, including the effect of currents.

The result of the above data processing is that each track is described in terms of athwartship position (y) and depth (z), relative to the vessel, and the time (t) before or after vessel–buoy passing. All tracks from all passings are compiled into a single data set, and this data set is used to estimate the model parameters. This results in more than 20 000 tracks of individual fish to estimate the parameters in the model.

Modelling individual trajectories

Let the stochastic variable $\boldsymbol{X}_t = (Y_t, Z_t)$ be the position of an individual at time t. The first component (Y_t) measures athwartship position, the second (Z_t) measures depth. The change in position (velocity) is modelled as the sum of a stochastic and a deterministic term:

$$(1)\qquad \frac{\mathrm{d}\boldsymbol{X}_t}{\mathrm{d}t} = \boldsymbol{U}_t + \boldsymbol{m}(z,t)$$

The deterministic term $\boldsymbol{m}(z,t)$ is the mean velocity for all individuals at a given depth z and time t. It is the average response to the vessel estimated using all vessel passings and was analysed in considerable detail in Handegard and Tjøstheim (2005). We have chosen to let $\boldsymbol{m}$ be independent of y; see explanation below. The stochastic term $\boldsymbol{U}_t$ represents the individual random deviation from the mean. Note that changes in velocity for a single individual are autocorrelated along its path, and consequently a simple Wiener process cannot be used to describe $\boldsymbol{U}_t$. We have chosen to use the OU process (see Cox and Miller (1970, pp. 225–228)) to model this behaviour, i.e.

$$(2)\qquad \mathrm{d}\boldsymbol{U}_t = -\mathbf{B}(z,t)\boldsymbol{U}_t\,\mathrm{d}t + \mathbf{S}(z,t)\,\mathrm{d}\boldsymbol{Z}(t)$$

where $\boldsymbol{Z}(t)$ is a two-dimensional Wiener process with zero mean, $\mathrm{cov}[Z_i(t), Z_j(s)] = 0$ for $i \neq j$, and $\mathrm{cov}[Z_i(t), Z_i(s)] = \min(t,s)$ for two time points t and s, and $i, j \in \{1,2\}$. Moreover

$$(3)\qquad \mathbf{B}(z,t) = \begin{bmatrix} \beta_{11}(z,t) & \beta_{12}(z,t) \\ \beta_{12}(z,t) & \beta_{22}(z,t) \end{bmatrix}$$

and

$$(4)\qquad \mathbf{S}(z,t) = \begin{bmatrix} \sigma_{11}(z,t) & \sigma_{12}(z,t) \\ \sigma_{12}(z,t) & \sigma_{22}(z,t) \end{bmatrix}$$

are parameters to be estimated from the data (see next section).

Once the parameters are estimated, simulated fish trajectories can be generated by integrating eqs. 1 and 2. We have used a simple forward scheme for this task. This is warranted by the relatively noisy data compared with the errors introduced using a simple forward scheme. The position at time step $k + 1$ is found using the position and velocity at time step k, the velocities are updated at the new position using eqs. 1 and 2, and the process is repeated. To initialize the simulations, an initial velocity $\boldsymbol{U}_{t_0} = \boldsymbol{u}_0$ and an initial position $\boldsymbol{X}_{t_0} = \boldsymbol{x}_0 = (y_0, z_0)$ are used. The initial velocities $\boldsymbol{u}_0$ are picked at random among tracks at t_0 and close to $\boldsymbol{x}_0$. The bottom and surface boundary are closed in the simulations, i.e., for a simulated fish at the boundary, with a simulated vertical velocity component that would bring the fish across the boundary, the vertical component is set to zero.

Estimating B and S from data

The fact that the process is decomposed into a mean model and a stochastic term (the OU process) has to be taken into account when estimating the parameters. We can remove the mean response by subtracting $\int_t^{t+\Delta t} \boldsymbol{m}(z,s)\,\mathrm{d}s$ from the fish track positions. Let the vector process $\boldsymbol{X}'(t) = [X_1'(t), X_2'(t)]$, where X_1 and X_2 denote the y and z components, respectively, consist of the residual positions $\boldsymbol{X}'(t + \Delta t) - \boldsymbol{X}'(t) = \boldsymbol{X}(t + \Delta t) - \boldsymbol{X}(t) - \int_t^{t+\Delta t} \boldsymbol{m}(z,s)\,\mathrm{d}s$. Note that t is the time for which the parameters $\mathbf{B}$ and $\mathbf{S}$ are estimated, and Δt is the time difference between t and subsequent positions along the tracks used in the estimation.

It is complicated to estimate the full $\mathbf{B}$ and $\mathbf{S}$ matrices as a function of $\boldsymbol{x} = (y,z)$ and t, and consequently, we make some simplifying assumptions. First, it has been found from the data processing that correlation between the changes in athwartship position $X_1'(t + \Delta t) - X_1'(t)$ and depth $X_2'(t + \Delta t) - X_2'(t)$ is weak (Appendix A), and we therefore neglect it. As a consequence, the off-diagonal terms β_{12} and σ_{12} of $\mathbf{B}$ and $\mathbf{S}$ in eqs. 3 and 4, respectively, are set to zero. The second simplifying assumption has to do with the poor resolution of the data in the athwartship direction (y). The tracks contain the athwartship position relative to the vessel, but since the buoy was passed at similar distances in the vessel–buoy experiments, the data are not resolved well in this direction. We have therefore chosen not to let the parameters β_{ii} and σ_{ii} vary as a function of y. Since our main interest is in the region close to $y = 0$, this approximation seems reasonable. These simplifications are further addressed in the Discussion. Finally, on the time scale of vessel passing (20 min), the duration of each track is short (typically 10 to 60 s). For each track at a given depth z and time t, we assume that β_{ii} and σ_{ii} are constant, or more precisely, for each track involved in the estimation of the parameters at a given z and t, we assume that $\mathbf{B}$ and $\mathbf{S}$ are constant.

To estimate the parameters of the OU process, we use $E\{\boldsymbol{X}'(t + \Delta t) - \boldsymbol{X}'(t)\} = 0$ and that for a one-dimensional OU process, here represented by $X_1'(t)$, with constant parameters β_{11} and σ_{11},

$$(5)\qquad E\{[X_1'(t + \Delta t) - X_1'(t)]^2\} = \frac{\sigma_{11}^2}{\beta_{11}^3}\{\beta_{11}(\Delta t) - 1 + \exp[-\beta_{11}(\Delta t)]\}$$

(Cox and Miller 1970, their eq. 106 on p. 228), and similarly for $X_2'(t)$. The left-hand side of eq. 5 can be estimated from the observations by subtracting the integrated mean term as already explained. The parameters σ_{ii} and β_{ii} on the right-hand side, representing the location–time (z,t), can then be estimated from eq. 5 by least squares analysis (details are given in Appendix A).

The probability of getting what you see

Let E_{eb} be the event that a fish is within the echo beam of the vessel when the centre of the vessel echo beam passes our fixed model plane, and let the event E_{tr} be the corresponding event of being available for the bottom trawl, i.e., being between the trawl door spread (50 m) and below the headline of the trawl (5 m) when the trawl doors pass the model plane. Note that we only consider fish behaviour before the arrival of the trawl doors. This configuration corresponds to the standard survey bottom trawl (Campelen 1800 shrimp trawl) used by the Institute of Marine Research (Bergen, Norway). The times for which these events occur are denoted $t = t_{\mathrm{eb}} = 0$ min and $t = t_{\mathrm{tr}} = 10$ min, respectively. Therefore, by definition, $t_{\mathrm{eb}} = 0$, and $t_{\mathrm{tr}} = 10$ min is the approximate time of trawl passage when trawling at 300 m depths.

If we initiate an individual fish, say, at $t_0 = -10$ min and $\boldsymbol{X}_{t_0} = (y_0, z_0) = (35, -280)$, we can simulate its path and determine for that individual whether the events E_{eb} or E_{tr} occur or not. When simulating several individuals for several initial locations, we can estimate the probability that these events occur as a function of t_0 and $\boldsymbol{x}_0$.

We have looked at two cases: one general case where $t_0 = -10$ min and a special case where we initialize our model at $t_0 = t_{eb} = 0$ min. The start time $t_0 = -10$ min corresponds to the time slightly after the vessel disturbs the fish, and $t_0 = t_{eb}$ corresponds to the time when we observe the fish on the echo sounder.

In the first case, we simulate N individuals starting at $\boldsymbol{X}_{t_0} = \boldsymbol{x}_0$, and we calculate the fraction of these individuals seen by the echo sounder (E_{eb}) and the fraction available to the trawl (E_{tr}). The probability is estimated by

$$(6) \qquad \widehat{P}\{E_{eb}|\boldsymbol{X}_{t_0} = \boldsymbol{x}_0\} = N_{eb}/N$$

where N is the total number of simulated individuals, and N_{eb} is the number of individuals within the echo beam at $t = t_{eb}$. Similarly,

$$(7) \qquad \widehat{P}\{E_{tr}|\boldsymbol{X}_{t_0} = \boldsymbol{x}_0\} = N_{tr}/N$$

Here N_{tr} is the number of simulated fish below the headline height and between the door spread, resulting in the probability of being available for the bottom trawl given the initial position $\boldsymbol{x}_0$. The simulations are performed for several $\boldsymbol{x}_0$ values to map the probabilities as a function of the initial position.

The second case is the probability of being available for the bottom trawl, given that the fish was seen on the echo sounder. This has special relevance, since there have been several attempts to find (or use) relations between the trawl catch and acoustic registrations (Aglen 1996; Hjellvik et al. 2003, 2007). Let E_{eb} and $Z_0 = z_0$ be the events of being within the beam and at a given initial depth z_0 at time $t_0 = t_{eb} = 0$. In this case, the initial positions are taken to be evenly distributed across the echo beam at the given depth. The probability of being available to the bottom trawl given that a fish was seen on the sounder at depth z_0 is estimated by

$$(8) \qquad \widehat{P}\{E_{tr}|E_{eb}, Z_0 = z_0\} = N_{tr}/N_{eb}$$

where N_{eb} is the total number of individuals, initially within the echo beam at $t_0 = t_{eb} = 0$ min and z_0 m depth, and N_{tr} is the number of these simulated individuals within the headline height and trawl door spread at trawl passing (t_{tr} = 10 min). The simulations are then performed for several start depths z_0 to estimate the probability to catch what you see as a function of depth.

Estimating the effective sampling volume

The parameters relating undisturbed biomass to trawl availability in the Dickson (1993*a*) model are k_{h3} and k_{v3}, where k_{h3} is the proportion of the vertical profile under the headline at the arrival of the trawl doors, and k_{v3} is the effect of horizontal behaviour. Dickson defines the fish between the doors and below the headline height as the number of

Fig. 4. The vertical profile from the buoy data fitted to the curve $g(z) = k_1/(z' + k_2) + k_3 z' + k_4$, where $z' = z + 300$ is height above bottom. The fitted parameters are $k_1 = 7.5 \times 10^{-2}$, $k_2 = 1.6$, $k_3 = -2.2 \times 10^{-5}$, and $k_4 = 5.3 \times 10^{-3}$. Negative values are set to zero. The grey and black curves show the mean profiles from the 2001 and 2002 experiments, respectively.

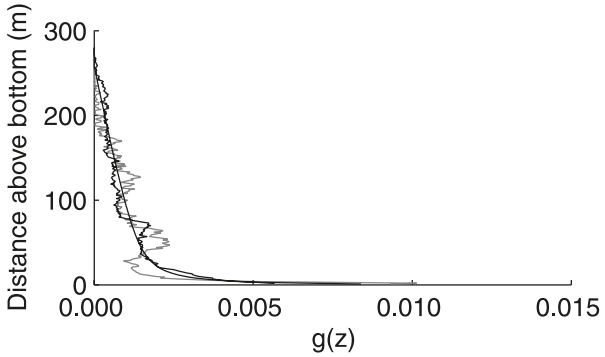

$$(9) \qquad \text{encounters} = y_b t_{tow} v \rho_a k_{h3} k_{v3}$$

(Dickson 1993*a*, his eq. 2), where y_b is trawl door spread (in our case y_b = 50 m), v is towing speed, t_{tow} is tow duration time, and ρ_a is (horizontal) area density. To interpret our results in the context of Dickson's effective sampling volume, we derive the number of encounters and the parameters k_{h3} and k_{v3} from our results.

The proportion of fish eventually under the headline and within the door spread is dependent both on behaviour and the undisturbed vertical density profile. Let

$$(10) \qquad \int_{z_d}^{0} f(z_0)\, \mathrm{d}z_0 + p_d = 1$$

where $f(z)$ is the vertical profile above the dead zone, z_d is the upper bound of the dead zone, and p_d is the proportion of fish in the dead zone. To be able to separate out the acoustic vertical profile in the calculations, we define

$$(11) \qquad g(z_0) = \frac{f(z_0)}{1 - p_d}$$

such that $\int_{z_d}^{0} g(z_0)\, \mathrm{d}z_0 = 1$. Here we use the mean vertical profile from the buoy data, excluding the passings, resulting in the scaled vertical profile $g(z_0)$ (Fig. 4). The proportion of fish in the dead zone is unknown, and we include the parameter p_d in the calculations to emphasize this. In the Discussion, various values of p_d are used to examine the implication of various proportions of fish in the dead zone.

The number of encounters using our approach is found by integrating the undisturbed density multiplied with the probability to be available to the trawl, i.e.

$$(12) \qquad N_{tr,A} = \rho_a t_{tow} v \left[(1 - p_d) \int_A g(z_0) P\{E_{tr}|\boldsymbol{X}_{t_0} = \boldsymbol{x}_0\}\, \mathrm{d}\boldsymbol{x}_0 + y_b p_d h_d \right]$$

where A is the area above the dead zone and below the surface, horizontally extending to infinity (in practice to where $P\{E_{\text{tr}}|\boldsymbol{X}_{t_0} = \boldsymbol{x}_0\}$ is zero), and h_{d} is a parameter related to the (unknown) behaviour in the fish that originally resided in the dead zone. Note that we assume that the detected behaviour is applicable to the fish that originally resided outside the dead zone, even if the reaction brings the fish into the dead zone during approach and passage of the vessel. The number of encounters for the hull-mounted echo sounder is

$$N_{\text{eb},A} = \rho_a t_{\text{tow}} v \left[(1 - p_{\text{d}}) \int_A g(z_0) P\{E_{\text{eb}}|\boldsymbol{X}_{t_0} = \boldsymbol{x}_0\} \, \text{d}\boldsymbol{x}_0 \right] \tag{13}$$

To get an idea of the implications of the observed behaviour in the presence of the vessel, we compute the numbers of encounters for trawl and acoustics assuming undisturbed fish and compare it with $N_{\text{tr},A}$ and $N_{\text{eb},A}$, respectively. Undisturbed encounters are computed by integrating the fish density within the trawl opening and echo beam at $t_0 = -10$ min. It is assumed by stationarity that the density will remain the same at time t_{tr} and t_{eb} and is calculated by

$$N^0_{\text{tr},A} = \rho_a t_{\text{tow}} v y_b \left[(1 - p_{\text{d}}) \int_{z_{\text{d}}}^{z_{\text{h}}} g(z_0) \, \text{d}z_0 + p_{\text{d}} \right] \tag{14}$$

where z_{h} is the headline height. Here we also assume stationarity for the fish in the dead zone by letting $h_{\text{d}} = 1$.

By equating eq. 9 with eqs. 12 and 14, we get

$$k_{h3} k_{v3} = \frac{(1 - p_{\text{d}})}{y_b} \int_A g(z_0) P\{E_{\text{tr}}|\boldsymbol{X}_{t_0} = \boldsymbol{x}_0\} \, \text{d}\boldsymbol{x}_0 + p_{\text{d}} h_{\text{d}} \tag{15}$$

for the disturbed case and

$$k_{v3} = \int_{z_{\text{d}}}^{z_{\text{h}}} (1 - p_{\text{d}}) g(z_0) \, \text{d}z_0 + p_{\text{d}} \tag{16}$$

for the undisturbed case, where $k_{h3} = 1$ by definition. These are used as estimates for the catchability parameters in Dickson's model. Note that both measures are dependent on p_{d}.

Results

Parameter estimation

Obtaining the estimate of the mean component $\boldsymbol{m}(z,t)$ is relatively straightforward. The result can be plotted directly and is easily interpreted. This was done in Handegard and Tjøstheim (2005). It is more difficult to interpret the estimated parameters for the stochastic parts, $\mathbf{B}(z,t)$ and $\mathbf{S}(z,t)$. To do this, we introduce a measure of the effective diffusion. For a small time step Δt, it is seen by series expansion of the exponential function in eq. 5 that the variance of the increments $X'_1(t + \Delta t) - X'_1(t)$ is proportional to $(\Delta t)^2$, but as $\Delta t \to \infty$, the variance is proportional to Δt, i.e.

$$\lim_{\Delta t \to \infty} E\{[(X'_1(t + \Delta t) - X'_1(t)]^2\} = \lim_{\Delta t \to \infty} \left\{ \frac{\sigma^2}{\beta^3} [\beta \Delta t - 1 + \exp(-\beta \Delta t)] \right\} = \frac{\sigma^2}{\beta^2} \Delta t \tag{17}$$

and similarly for X'_2. Then σ^2/β^2 represents a measure of how quickly the probability density diffuses at large Δt. In practice, this is valid for approximately $\Delta t > 2$ min (see Appendix A).

The parameter estimates themselves are obtained by fitting the curve in eq. 5 to the empirical data (see Appendix A and in particular Fig. A1). The estimates of $\boldsymbol{m}$ and the ratios $\widehat{\sigma}^2_{ii}/\widehat{\beta}^2_{ii}$ (effective diffusion) are shown as a function of time and depth (Fig. 5). The gross features for $\boldsymbol{m}$ are the same as in Handegard and Tjøstheim (2005, cf. their fig. 7). The vertical component m_2 is slightly negative around 10 min before vessel passing. The strongest and sharpest response is related to the trawl warps, where a strong avoidance is seen in front of the warps. Note also that the vertical effective diffusion is reduced when the magnitude of the mean component increases, between 5 and 10 min after vessel passage, indicating a more directional movement. This movement was attributed to a directional response away from the warps. Note also that the horizontal diffusion is close to two orders of magnitude higher than the vertical diffusion.

To evaluate the effect of the different levels of smoothing, a table of the estimated mean effective diffusion $\widehat{\sigma}^2_{ii}/\widehat{\beta}^2_{ii}$ is given (Table 1) for the random movement in both the horizontal (y) and vertical (z) directions. In the table $\Delta t_{\max}$ is the maximum Δt used in the fitting of the curve in eq. 5 to empirical data. For example, in Fig. A1 $\Delta t_{\max} = 60$. It is seen from the table that different levels of smoothing have little impact of the estimated ratio $\widehat{\sigma}^2_{ii}/\widehat{\beta}^2_{ii}$.

Computing probabilities with the OU model

Here the results from the two case studies are presented. In case 1, the objective is to map the probability for a fish to be seen on the echo sounder and to be available for the bottom trawl, given a starting position $\boldsymbol{x}_0$ at $t_0 = -10$ min. In case 2, we are interested in the probability that a fish is available for the bottom trawl given that it was seen on the echo sounder at depth z_0 and $t_0 = t_{\text{eb}}$. In both cases, an example for one initial position $\boldsymbol{x}_0$ or z_0 is given, before presenting the result as a function of $\boldsymbol{x}_0$ or z_0.

First we present the result for one initial position for case 1. We simulated $N = 40$ individuals with initial position $\boldsymbol{x}_0 = (35, -280)$, i.e., 35 m off the vessel path to starboard, at 280 m depth, and initial time $t_0 = -10$ (Figs. 6 and 7). The objective of these figures is to explain how the probabilities $P\{E_{\text{eb}}|\boldsymbol{X}_{t_0} = \boldsymbol{x}_0\}$ and $P\{E_{\text{tr}}|\boldsymbol{X}_{t_0} = \boldsymbol{x}_0\}$ are estimated using eqs. 6 and 7 for a single initial position. The number of individuals within the echo beam at $t = t_{\text{eb}} = 0$ are counted (Fig. 6) and divided by $N = 40$. Note that this estimated probability may be different from the final estimated probabilities because of the low numbers of realizations in this example run. Similarly, the numbers of individuals below the trawl headline and between the door spread are counted at $t = t_{\text{tr}} = 10$ min (Fig. 7).

Fig. 5. The mean velocity of all tracks, $\widehat{m}_1$ (horizontal velocity) and $\widehat{m}_2$ (vertical velocity), where $\widehat{\boldsymbol{m}} = (\widehat{m}_1, \widehat{m}_2)$ are shown in panels (*a*) and (*b*), respectively, and the effective diffusion in the horizontal direction ($\widehat{\sigma}^2_{11}/\widehat{\beta}^2_{11}$) and in the vertical direction ($\widehat{\sigma}^2_{22}/\widehat{\beta}^2_{22}$), are shown in panels (*c*) and (*d*), respectively. All parameters are resolved in depth (z) and time before (negative t) and after (positive t) vessel passing. "T'' on the x axes denotes trawl passage. The athwartship dependence (y) is ignored. A strong horizontal swimming away from the transducer is seen after the passage of the vessel (I), and an initial weak diving (II) is followed by a strong diving when the trawl warps passes (III). The effective diffusion is relatively stable, except for a strong signal in the horizontal diffusion just after trawl warp passage (IV), indicating a less directional movement. The vertical diffusion (V) is stronger before and after trawl warp passing, indicating a directional movement closer to the warps.

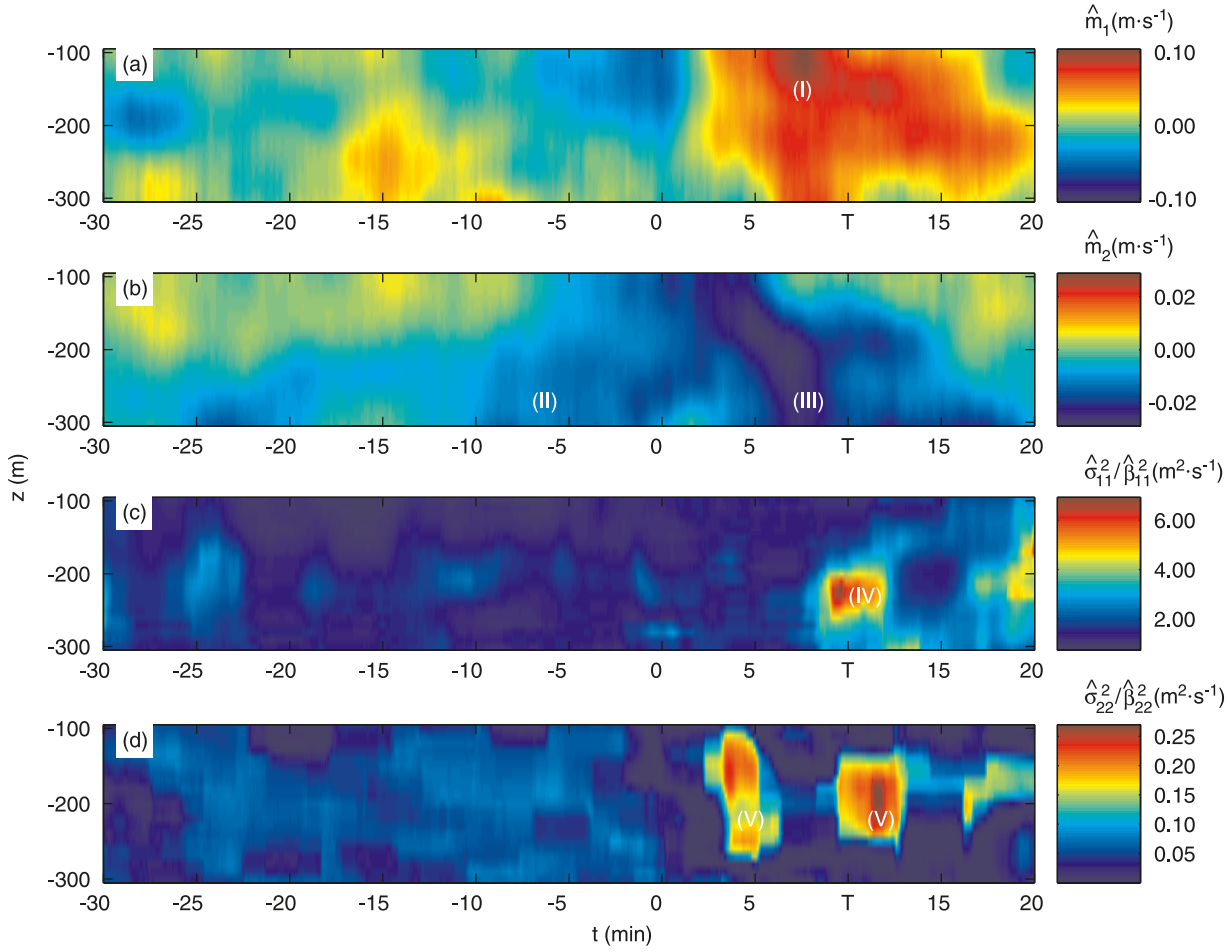

Repeating this procedure for a wide range of initial positions enable us to contour the probability as a function of $\boldsymbol{x}_0$. The initial positions used were y_0 from 0 to 100 m in steps of 5 m and z_0 from –300 to –250 m in steps of 5 m (all combinations) for E_{tr} and y_0 from 0 to 100 m in steps of 5 m and z_0 from –300 to 0 m in steps of 20 m for E_{eb} (all combinations). For each initial position, we simulated N = 5000 individuals. This number gave fairly smooth contours. The estimated probabilities $\widehat{P}\{E_{\text{eb}}|\boldsymbol{X}_{t_0} = \boldsymbol{x}_0\}$ and $\widehat{P}\{E_{\text{tr}}|\boldsymbol{X}_{t_0} = \boldsymbol{x}_0\}$ are presented as a function of $\boldsymbol{x}_0$ (Fig. 8). Note that the probabilities extend farther horizontally than vertically for $\widehat{P}\{E_{\text{tr}}|\boldsymbol{X}_{t_0} = \boldsymbol{x}_0\}$ (Fig. 8*b*), indicating a higher activity in the horizontal direction (consistent with Fig. 5 and Table 1) than in the vertical one.

In case 2 we are particularly interested in the probability that a fish is available for the bottom trawl given that it was seen on the echo sounder at depth z_0 and $t_0 = 0$. This corresponds to the probability $P\{E_{\text{tr}}|E_{\text{eb}}, Z_0 = z_0\}$, as estimated by eq. 8. Similar to case 1, we first present an example from a small number of particles. We simulated 40 individuals with initial time t_0 = t_{eb} = 0, initially located at depth z = –285 m inside the echo beam (the event E_{eb}), approximated by four initial positions evenly distributed across the echo beam at the given depth. The particles that end up as available to the trawl at t = 10 min are counted and used as an estimate for $P\{E_{\text{tr}}|E_{\text{eb}}, Z_0 = z_0\}$ (Fig. 9). Again, note that this probability estimate will in general be different from the final simulated probabilities because of the low numbers of realizations in the example run.

Similar to case 1, we repeat the procedure, but now for several different depths z_0, from –300 to –250 m in uniform steps of 5 m. The corresponding estimated probability of being available to the bottom trawl, given it was registered in the echo sounder, $\widehat{P}\{E_{\text{tr}}|E_{\text{eb}}, Z_0 = z_0\}$, is presented as a function of z_0 (Fig. 10). Note that the maximum probability

Table 1. The estimated effective diffusion in the horizontal direction ($\widehat{\sigma}^2_{11}/\widehat{\beta}^2_{11}$) and in the vertical direction ($\widehat{\sigma}^2_{22}/\widehat{\beta}^2_{22}$) for different levels of smoothing and different track lengths in the estimation (Δt_{max}).

	Δt_{max} = 40	Δt_{max} = 60	Δt_{max} = 100
Horizontal ($\widehat{\sigma}^2_{11}/\widehat{\beta}^2_{11}$)			
SP spar = 0.3	1.201	1.434	1.555
SP spar = 0.5	1.304	1.523	1.514
SP spar = 0.7	1.633	1.814	1.635
SP spar = 0.9	2.123	2.076	1.712
SNP	1.399	1.583	1.515
KS	1.576	1.703	1.556
Vertical ($\widehat{\sigma}^2_{22}/\widehat{\beta}^2_{22}$)			
SP spar = 0.3	0.057	0.053	0.043
SP spar = 0.5	0.060	0.053	0.039
SP spar = 0.7	0.067	0.055	0.037
SP spar = 0.9	0.067	0.055	0.034
SNP	0.061	0.053	0.038
KS	0.063	0.055	0.037

Note: SP, parametric splines with four different levels of smoothing; SNP, nonparametric splines with cross validation; KS, Kalman smoothing.

Fig. 6. The results when simulating 40 individuals starting at a single initial position (◇) at t_0 = –10 min. The resulting particle positions (asterisks) at t = 0 min and the corresponding estimate of $\widehat{P}\{E_{eb}|\boldsymbol{X}_{t_0} = \boldsymbol{x}_0\} = 0.32$ are shown. The slanted vertical lines are the outline of the echo beam (8° beam opening). To view the video, see the HTML Web version of this paper at cjfas.nrc.ca.

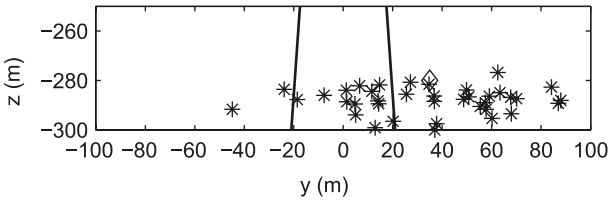

Fig. 7. The results when simulating 40 individuals starting at a single initial position (◇) at t_0 = –10 min. The resulting positions at t = 10 min (asterisks) and the associated probability $P\{E_{tr}|\boldsymbol{X}_{t_0} = \boldsymbol{x}_0\} = 0.17$ are shown. The solid lines in the lower part of the plot denote the doorspread (50 m) and headline height (5 m) of the trawl. To view the video, see the HTML Web version of this paper at cjfas.nrc.ca.

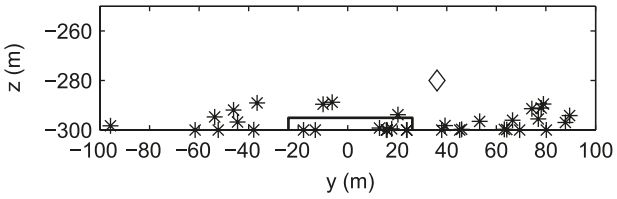

is about 0.35, indicating that there is a relatively low probability to be available to the trawl if the fish initially is at the bottom and seen by the echo sounder. This is attributed to the large lateral displacement.

Estimating encounters

Based on the model, the typical vertical profile (Fig. 4),

Fig. 8. The estimated probabilities $\widehat{P}\{E_{eb} \mid \boldsymbol{X}_{t_0} = \boldsymbol{x}_0\}$ (panel *a*) and $\widehat{P}\{E_{tr} \mid \boldsymbol{X}_{t_0} = \boldsymbol{x}_0\}$ (panel *b*) as a function of the initial position $\boldsymbol{x}_0 = (y_0, z_0)$. The diamond (◇) show the initial position from the example run in Figs. 6 and 7.

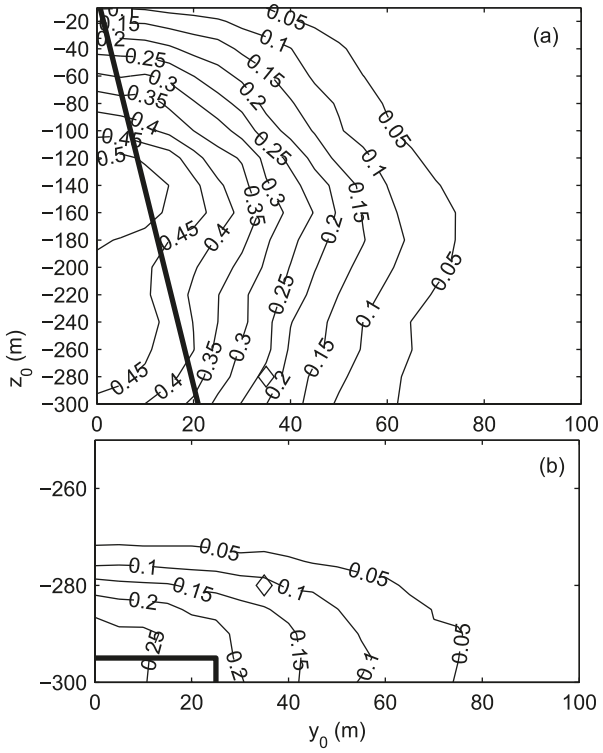

and the assumed unknown proportion (p_d) and behaviour (h_d) of fish in the dead zone, we express the number of encounters for the trawl and echo sounder using eqs. 12 and 13 as

$$(18) \qquad N_{tr,A} = \rho_a t_{tow} v[(1 - p_d)8.4 + 50\ p_d h_d]$$

and the number of echo beam encounters as

$$(19) \qquad N_{eb,A} = \rho_a t_{tow} v(1 - p_d)37$$

The numbers 8.4 and 37 are the numerical values of the integrals in eqs. 12 and 13, respectively, and 50 is the trawl door spread.

Assuming no fish disturbance (eq. 14), we get the number of trawl encounters

$$(20) \qquad N^0_{tr,A} = \rho_a t_{tow} v\ 50[7.58(1 - p_d) + p_d]$$

for the stationary case. Here, 7.58 and 50 are the numerical values of the integral in eq. 14 and the trawl door spread, respectively.

The parameters for Dickson's trawl model are then estimated as $k_{v3}k_{h3} = 0.17(1 - p_d) + p_d h_d$ and $k_{v3}k_{h3} = 0.15 + p_d$ for the disturbed (eq. 15) and stationary (eq. 16) cases, respectively.

Assuming p_d = 0.2 (which is probably too high; O.R. Godø, Institute of Marine Research, P.O. Box 1870, Nordnes, 5817 Bergen, Norway, personal communication; see also Hjellvik et al. 2004) and h_d = 1 (stationary behaviour for the fish in the dead zone), we get $N_{tr,A} = 16.8\rho_a t_{tow} v$ and $N^0_{tr,A} = 16.1\rho_a t_{tow} v$ for the disturbed and stationary cases, respectively. Using the same assumptions, the Dick-

Fig. 9. Four initial positions, each containing five individuals across the echo beam at $t = 0$, are shown as diamonds ($\diamond$), with the resulting particle positions at $t = 10$ min shown as asterisks (*), and the associated estimated probability $\widehat{P}\{E_{\text{tr}}|E_{\text{eb}}, Z_{t_0} = -285\} = 0.2$. To view the video, see the HTML Web version of this paper at cjfas.nrc.ca.

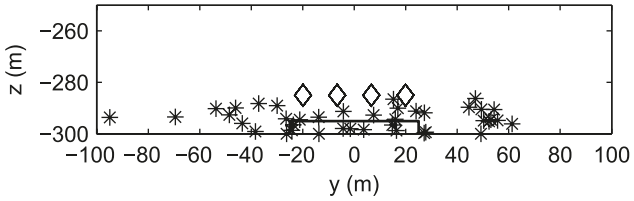

son parameters are $k_{v3}k_{h3} = 0.34$ and $k_{v3}k_{h3} = 0.32$ for the disturbed and stationary cases, respectively.

Discussion

The discussion section has two main parts. In the first part we discuss the method, including the choice of model, the parameter estimation procedure, the simplifications, etc. The data material and tracking method are not discussed in detail, since they are quite thoroughly described in Handegard and Tjøstheim (2005) and Handegard et al. (2005), respectively. In the second part, the focus is on potential applications, relating our work to catchability in general and to the Barents Sea winter survey case in particular. This is relevant for fish abundance estimation.

The choice of model, parameter estimation, and data material

We have used the OU process to model the stochastic part of the simulated fish trajectories, but there are other possibilities. One alternative choice is the Wiener process, where it is assumed that changes in the motion of the particles are independent from one time step to the next. These types of models have successfully been used to fit tagging data for larger-scale movement processes, see e.g., Sibert et al. (1999) or Sparrevohn et al. (2002). Lévy flights are another class of random-walk models whose step lengths are chosen from a probability distribution with a power-law tail. These have been used to model search patterns for, e.g., albatrosses (Viswanathan et al. 1996), but the generality of the Lévy assumption has recently been questioned (Edwards et al. 2007).

We have chosen the OU process, because the autocorrelation curve from the OU process gives a much better data fit than the corresponding curve for the Wiener process. The reason for the better fit is that the fish trajectory has correlated increments, and fitting a Wiener process that has non-correlated increments does not work well. The OU model implies that each fish (particle) has a mass (and inertia), and consequently an along-track correlation. Moreover, the OU approach assumes random impulses on the acceleration instead of on the velocity.

Although the OU model seems to be the more appropriate choice, the variance of the Wiener process and OU process are both proportional to $t - t_0$ for large values of $t - t_0$, indicating that for a long model run time, the trajectories could be simulated by the less computationally demanding Wiener process, giving approximately the same result. The parameter estimation technique, however, would then have to be adjusted to compensate for the along-track correlation.

Fig. 10. The estimated probability $\widehat{P}\{E_{\text{tr}}|E_{\text{eb}}, Z_{t_0} = z_0\}$ as a function of z_0.

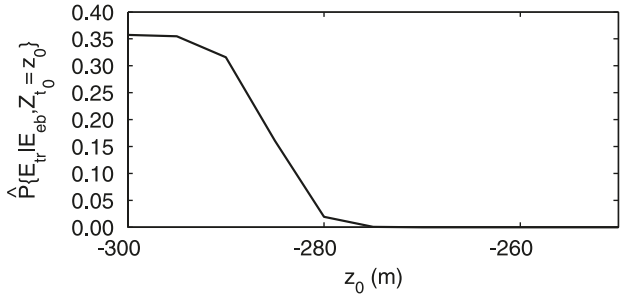

A consequence of assuming a diffusion approximation as represented by the OU model is that the fish will continue to spread (diffuse) as $t - t_0$ gets large. In some cases, the fish has a preferred depth and location, and our model does not capture this. The preferred depth could, for example, be modelled by an advection term directed towards the preferred location. Another way to restrict the diffusion would be to let the along-track autocorrelation curve be negative for some values of $t - t_0$ (Okubo 1986, his fig. 2). However, we assume that these processes occur on a different time scale than the buoy–vessel-passing time scale, and since the data do not suggest another functional form of this curve, we argue that the OU model is appropriate in our case.

In an earlier version of the paper, we computed a backward-propagating solution using the Kolmogorov backward formulation based on the diffusion equation for the density (Cox and Miller 1970, sec. 5.6). Reformulating the problem to a density model has the advantage that the result will be independent of the number of individuals in the simulations. Running the model backwards is also appealing because a single model run would give us the probability map of availability to the trawl. The reason for abandoning this approach was twofold. First, a density model requires solving numerically a set of partial differential equations, and in a few cases divergence and instability occurred. When running the model backwards, there is also the issue of boundary conditions. Since the advection brings the fish towards the bottom, a lot of density is held at the bottom channel when running forward. When we run it backward, this density is lifted off the bottom by the advection, giving room for the diffusion to work. We have not studied this extensively, but together with the above-mentioned concerns, we abandoned the density model and chose the particle model based on the stochastic differential eq. 2 instead. Another advantage with the particle model is that more complex, individual-based behaviour is simpler to include.

No dependence between individuals is assumed in this model. This may be approximately true for species like Atlantic cod and haddock, but is clearly not valid for schooling pelagic species like, e.g., Atlantic herring and mackerel (*Scomber scombrus*). Correlation between individuals can easily be implemented in an individual-based model. The simplest approach would be to separate the stochastic term, $\boldsymbol{Z}(t)$ in eq. 2 into two separate terms: one for each individual and one common for all individuals. More sophisticated approaches could also be thought of, where zones of attraction, repulsion, and polarisation could be defined (Aoki 1982; Reynolds 1987; Huth and Wissel 1992). Such an approach could

give an indication of the importance of schooling by estimating the degree of common movement as a value of a parameter. Ideally, this should be estimated for different species, and then simulations could be carried out to investigate the difference in catchability for these species. Since we lack the data for such a study, and since demersals do not display strong schooling behaviour, we have chosen not to implement it in this paper.

The effective diffusion defined in eq. 17 is surprisingly insensitive to the degree of smoothing. The reason for this is that the effective diffusion is dependent on the speed and the rate of directional change (along-track correlation) of the individuals (Okubo 1986, his eq. III.12). If the smoothing is low, the curved paths lead to high speed estimates, but low along track correlation estimates, and vice versa. These effects cancel each other and explain the low dependence on the strength of the smoothing operator.

The model is based on a projection of fish movement onto the athwartship–depth plane, ignoring the alongship dimension. This is warranted by the large difference in vessel speed (1.5 $m \cdot s^{-1}$) compared with the mean in the alongship velocity component of the fish, which varies between 0 and 0.03 $m \cdot s^{-1}$ (Handegard and Tjøstheim 2005, their fig. 1*a*). If we further assume that the diffusion along the alongship axis varies slowly and that the fish density is fairly uniform, the net number of fish that are brought in or out of the model plane by diffusion is close to zero. A total model run time of 20 min with a mean speed of 0.03 $m \cdot s^{-1}$ will transport the fish 36 m. As a comparison, the vessel travels 1800 m in the same time interval.

There are two reasons for ignoring the parameter dependence on the athwartship coordinate y. First, the data is not resolved well in y, and second, an assumed dependence had neglible effect on the result. More precisely, we initially assumed a Gaussian weight function on the parameters as a function of y, but since the relevant processes occur close to the trawl and vessel, reducing the vessel effect at a distance had virtually no influence on the final result.

A problem using acoustics, both for behavioural observations and echo integration, is the acoustic dead zone close to the bottom (Ona and Mitson 1996). Defining catchability coefficients will be erroneous without addressing the dead zone problem. We have circumvented this by including a undetectable proportion p_d of the fish population in the dead zone. It is also worth noting that we do not consider altered behaviour in the nondetectable portion of the water column, although we do recognize that portions of the initially detectable fish swim into the dead zone. If the behaviour during that process is dramatically changed, it will introduce a bias.

Applications

We have been able, based on a model with parameters estimated from data, to compute a probability map describing where the fish available to the trawl are coming from, and we have estimated the probability that a fish detected by the echo sounder at a given depth is available to the trawl. For a discussion of the observed average reaction pattern, we refer again to the discussion in Handegard and Tjøstheim (2005).

For the vertical profile depicted in Fig. 4, and with the assumptions described in the Materials and methods section, the ratio $N_{tr,A}/N_{eb,A} = [(1 - p_d)8.4 + 50 p_d h_d]/[(1 - p_d)37]$ (from eqs. 18 and 19) indicates the relative efficiency between trawl and acoustic based on that vertical profile and our model assumption.

In the extreme case of no fish in the acoustic dead zone, the acoustic system encounters four times as many fish as the trawl ($p_d = 0$ yields $N_{tr,A}/N_{eb,A} = 0.23$). If we postulate the same numbers of encounters in both systems ($N_{tr,A} = N_{eb,A}$), we may equate eqs. 18 and 19 and solve for p_d. Assuming $h_d = 1$, we get $p_d = 0.36$. This means that 36% of the fish must be found in the acoustic dead zone for the trawl to encounter more fish than the acoustic system, which is unrealistic. Consequently, the acoustic system detects a larger fraction of the stock. However, there is in general lower error residuals for trawl indices than the acoustic indices in the Barents Sea compared with the assessment models (ICES 2008, their fig. 3.5). Assuming that our results hold true, these discrepancies are not caused by lower availability to the acoustic system than to the trawl.

We have shown how observations of swimming trajectories can be used to determine parameters of trawl efficiency models, using Dickson's (1993*a*) model as an example. Using the vertical profile for the Barents Sea experiment, we obtained $k_{h3}k_{v3} = 0.17(1 - p_d) + p_d h_d$. This is quite low unless there is a substantial part of the biomass in the dead zone. Comparing this result with the undisturbed case, we get $k_{v3} = 0.15 + p_d(k_{h3} = 1)$, i.e., quite similar for p_d values around 0.1. The catchability is quite similar for these two situations, even if there is vertical herding when assuming nonstationary fish. Consequently, horizontal behaviour is important. We gain fish by vertical herding and lose fish through horizontal escapement.

The typical fishing height predicted by our model is lower than those of previous studies (Aglen 1996; Hjellvik et al. 2003). They rely on the correlation between the converted catches to acoustic density and the cumulative echo energy up to a certain height above bottom. The height above bottom where the correlation peaked was taken as the typical fishing height of the trawl. The peak varied between 10 and 50 m, depending on species, day–night, year, etc., but the correlation was generally low. Hjellvik et al. (2003) also tried to fit a catchability function to the data, where the catchability decreases with depth above bottom (their fig. 6), but the fit was generally poor. There may be several reasons for the discrepancy between our results and theirs. First, the definitions are different. They rely on correlations, whereas we rely on probability statements and simulations. Second, we use a different data set. Third, we may lose fast-swimming fish in the tracking, resulting in an underestimate of the vertical advection and consequently underestimate the fishing height.

If we use the typical vertical profile to initialize our model at $t = 0$ (i.e., assume that the undisturbed vertical profile is valid for vessel passage) and calculate the probability for a fish being available to the trawl when seen on the sounder, we get

$$\frac{\int_{z_0=-300}^{0} g(z_0)\widehat{P}\{E_{tr}|E_{eb}, Z_{t_0} = z_0\}\, dz_0}{\int_{z_0=-300}^{0} g(z_0)\, dz_0} = 0.092$$

This number is low and may explain the low correlation be-

tween catch and acoustics in the previous works. This effect would be less pronounced if the horizontal distribution is uniform. Then the correlation between trawl and acoustics may increase, since you are not required to catch exactly the fish you see.

In both of the above cases, vertical herding and horizontal avoidance play a critical role. In the traditional approach, it is (correctly) assumed that fish are herded downwards, but the reduction of fish available due to horizontal movement out of the trawl path is not recognized. This is consistent with the increased efficiency of industrial pair trawling.

Perspectives

Our approach does not separate between different size groups and species, which is especially important when using the survey data for relative indices of abundance. Moreover, we have not stratified our data on different years and locations, etc. Initially this was tried, but with no clear-cut results (Handegard 2004, paper IV). One explanation may be that the available data set is too small and too noisy to separate these effects from the general trend. The fish response to the vessel and gear may be highly variable, dependent on the fish motivation. The motivation may change based on predator presence, prey availability, etc. (Pitcher 1993), causing further variability. This may result in different reaction patterns between years and is named the "survey condition" in Godø and Wespestad (1993). Consequently, investigating the variable effect is more important than the mean effect when using the survey data as annual indices of abundance. For estimates of absolute abundance, however, the absolute observation volume is necessary to relate catch to density.

We have shown how the data from experiments can be translated into parameters important for the survey. We have also shown the implications of the observed reaction pattern. To go from here to an estimate of absolute abundance, the challenge is to design methods to continuously monitor or evaluate the validity of the model results. In a similar way that echo sounders are calibrated, the fish behaviour needs to be calibrated. This is not the main focus in this paper, but it is hoped that our results could promote further progress along the lines of absolute abundance estimation. For a more thorough discussion of this point, we refer to Handegard (2004, pp. 20–24).

Acknowledgements

We are grateful to Alex De Robertis and Frode Vikebø for useful comments on the manuscript. We are also grateful to an anonymous referee that substantially improved our manuscript. The work was supported under the Norwegian Research Council, under the "Leiv Erikson mobilitetsprogram" and the strategic institute programs "Absolute Abundance Estimation of Fish" and "Ecosystem Dynamics and Fish Stocks".

References

Aglen, A. 1996. Impact of fish distribution and species composition on the relationship between acoustic and swept-area estimates of fish density. ICES J. Mar. Sci. **53**: 501–506. doi:10.1006/jmsc.1996.0072.

Aglen, A., Engås, A., Huse, I., Michalsen, K., and Stensholt, B.K. 1999. How vertical distribution may affect survey results. ICES J. Mar. Sci. **56**: 345–360. doi:10.1006/jmsc.1999.0449.

Aoki, I. 1982. A simulation study on the schooling mechanism in fish. Bull. Jpn. Soc. Sci. Fish. **48**(8): 1081–1088.

Cox, D., and Miller, H. 1970. The theory of stochastic processes. Methuen & Co. Ltd., London, UK.

De Robertis, A., and Wilson, C.D. 2006. Walleye pollock respond to trawling vessels. ICES J. Mar. Sci. **63**: 514–522. doi:10.1016/j.icesjms.2005.08.014.

Dickson, W. 1993*a*. Estimation of the capture efficiency of trawl gear. I: Development of a theoretical model. Fish. Res. **16**: 239–253. doi:10.1016/0165-7836(93)90096-P.

Dickson, W. 1993*b*. Estimation of the capture efficiency of trawl gear. II: Testing a theoretical model. Fish. Res. **16**: 255–272. doi:10.1016/0165-7836(93)90097-Q.

Edwards, A.M., Phillips, R.A., Watkins, N.W.Freeman, M.P.Murphy, E.J. Afanasyev, V. Buldyrev, S.V. da Luz, M.G.E. Raposo, E.P. Stanley, H.E., and Viswanathan, G.M. 2007. Revisiting levy flight search patterns of wandering albatrosses, bumblebees and deer. Nature (London), **449**(7165): 1044–1048. ISSN 0028-0836.

Engås, A., and Godø, O.R. 1989. Escape of fish under the fishing line of a Norwegian sampling trawl and its influence on survey results. ICES J. Mar. Sci. **45**(3): 269–276. doi:10.1093/icesjms/45.3.269.

Engås, A., Godø, O.R., and Jørgensen, T. 2000. A comparison between vessel and trawl tracks as observed by the ITI trawl instrumentation. Fish. Res. **45**: 297–301. doi:10.1016/S0165-7836(99)00123-X.

Fernandes, P.G., Brierley, A.S., Simmonds, E.J., Millard, N.W., McPhail, S.D., Armstrong, F., Stevenson, P., and Squires, M. 2000*a*. Fish do not avoid survey vessels. Nature (London), **404**: 35–36. doi:10.1038/35003648. PMID:10716432.

Fernandes, P.G., Brierley, A.S, Simmonds, E.J., Millard, N.W., McPhail, S.D., Armstrong, F., Stevenson, P., and Squires, M. 2000*b*. Addendum: Fish do not avoid survey vessels. Nature (London), **407**: 152. doi:10.1038/35025149.

Godø, O.R., and Wespestad, V. 1993. Monitoring changes in abundance of gadoids with varying availability to trawl and acoustic surveys. ICES J. Mar. Sci. **50**: 39–51. doi:10.1006/jmsc.1993.1005.

Handegard, N.O. 2004. Cod reaction to an approaching bottom trawling vessel investigated using acoustic split-beam tracking. Ph.D. thesis, Department of Mathematics, University of Bergen, Bergen, Norway.

Handegard, N.O., and Tjøstheim, D. 2005. When fish meets a trawling vessel: examining the behaviour of gadoids using a free floating buoy and acoustic split-beam tracking. Can. J. Fish. Aquat. Sci. **62**: 2409–2422. doi:10.1139/f05-131.

Handegard, N.O., Michalsen, K., and Tjøstheim, D. 2003. Avoidance behaviour in cod (*Gadus morhua*) to a bottom-trawling vessel. Aquat. Living Resour. **16**: 265–270. doi:10.1016/S0990-7440(03)00020-2.

Handegard, N.O., Patel, R., and Hjellvik, V. 2005. Tracking individual fish from a moving platform using a split-beam transducer. J. Acoust. Soc. Am. **118**(4): 2210–2223. doi:10.1121/1.2011410. PMID:16266143.

Hjellvik, V., Michalsen, K., Aglen, A., and Nakken, O. 2003. An attempt at estimating the effective fishing height of the bottom trawl using acoustic survey recordings. ICES J. Mar. Sci. **60**: 967–979. doi:10.1016/S1054-3139(03)00116-4.

Hjellvik, V., Godø, O.R., and Tjøstheim, D. 2004. Diurnal variation in acoustic densities: why do we see less in the dark? Can. J. Fish. Aquat. Sci. **61**(11): 2237–2254. doi:10.1139/f04-161.

Hjellvik, V., Tjøstheim, D., and Godø, O.R. 2007. Can the precision of bottom trawl indices be increased by using simultaneously collected acoustic data? The Barents Sea experience. Can. J. Fish. Aquat. Sci. **64**: 1390–1402. doi:10.1139/F07-101.

Huth, A., and Wissel, C. 1992. The simulation of the movement of fish schools. J. Theor. Biol. **156**: 365–385. doi:10.1016/S0022-5193(05)80681-2.

ICES. 2008. Report of the Arctic Fisheries Working Group (AFWG). Available from www.ices.dk/reports/ACOM/2008/AFWG/directory.asp.

Løland, A., Aldrin, M., Ona, E., Hjellvik, V., and Holst, J.C. 2007. Estimating and decomposing total uncertainty for survey-based abundance estimates of Norwegian spring-spawning herring. ICES J. Mar. Sci. **64**: 1302–1312. doi:10.1093/icesjms/fsm116.

Nunnallee, E.P. 1991. An investigation of the avoidance reactions of pacific whiting (*Merluccius productus*) to demersal and midwater trawl gear. ICES CM 1991/B:5.

Okonski, S. 1969. Echo sounding observations of fish behaviour in the proximity of the trawl. FAO Fish. Rep. **62**(2): 377–388.

Okubo, A. 1986. Dynamical aspects of animal grouping: swarms, schools, flocks and herds. Adv. Biophys. **22**: 1–94. doi:10.1016/0065-227X(86)90003-1. PMID:3551519.

Olsen, K., Angell, J., Pettersen, F., and Løvik, A. 1983. Observed fish reactions to a surveying vessel with special reference to herring, cod, capelin and polar cod. FAO Fish. Rep. **300**: 131–138.

Ona, E., and Godø, O.R. 1990. Fish reaction to trawling noise: the significance for trawl sampling. Rapp. P.-V. Reun. Cons. Int. Explor. Mer, **189**: 159–166.

Ona, E., and Mitson, R. 1996. Acoustic sampling near the seabed: the deadzone revisited. ICES J. Mar. Sci. **53**: 677–690. doi:10.1006/jmsc.1996.0087.

Ona, E., Godø, O.R., Handegard, N.O., Hjellvik, V., Patel, R., and Pedersen, G. 2007. Silent research vessels are not quiet. J. Acoust. Soc. Am. **121**: EL145–EL150. doi:10.1121/1.2710741. PMID:17471759.

Pitcher, T.J. (*Editor*). 1993. Behaviour of teleost fishes. Vol. 7. Chapman and Hall Fisheries Series. 2nd ed. Chapman and Hall, London, UK.

Ramm, D.C., and Xiao, Y. 1995. Herding in groundfish and effective pathwidth of trawls. Fish. Res. **24**: 243–259. doi:10.1016/0165-7836(95)00373-I.

Reynolds, C.W. 1987. Flocks, herds, and schools: a distributed behavioural model. Comput. Graph. (ACM), **21**(4): 25–34. doi:10.1145/37402.37406.

Sibert, J.R., Hampton, J., Fournier, D.A., and Bills, P.J. 1999. An advection–diffusion–reaction model for the estimation of fish movement parameters from tagging data, with application to skipjack tuna (*Katsuwonus pelamis*). Can. J. Fish. Aquat. Sci. **56**: 925–938. doi:10.1139/cjfas-56-6-925.

Sparrevohn, C.R., Nielsen, A., and Støttrup, J.G. 2002. Diffusion of fish from a single release point. Can. J. Fish. Aquat. Sci. **59**: 844–853. doi:10.1139/f02-059.

Vabø, R., Olsen, K., and Huse, I. 2002. The effect of vessel avoidance of wintering Norwegian spring spawning herring. Fish. Res. **58**: 59–77. doi:10.1016/S0165-7836(01)00360-5.

Viswanathan, G.M., Afanasyev, V., Buldyrev, S.V., Murphy, E.J., Prince, P.A., and Stanley, H.E. 1996. Levy flight search patterns of wandering albatrosses. Nature (London), **381**(6581): 413–415. doi:10.1038/381413a0.

List of symbols

$\boldsymbol{x} = (y, z)$ model coordinates (upwards is positive z)
x alongship direction (not used in the model)
t time before or after vessel passing; negative time is before passing
v vessel speed
$\boldsymbol{X}_{t_k} = (Y_{t_k}, Z_{t_k}) = [X_1(t_k), X_2(t_k)]$; stochastic variable of the fish position
$\boldsymbol{X}'_{t_k} = (Y'_{t_k}, Z'_{t_k}) = [X'_1(t_k), X'_2(t_k)]$; stochastic variable of the fish position without the mean drift
$\boldsymbol{U}_t$ individual random deviation from the mean velocity
$\boldsymbol{m} = (m_1, m_2)$ the mean fish velocity (advection)
$\boldsymbol{Z}(t)$ two-dimensional (2D) Wiener process
$\mathbf{B}(z,t)$ Ornstein–Uhlenbeck (OU) parameter matrix for the velocity correlation
β_{ij} elements of B
$\mathbf{S}(z,t)$ OU parameter for the random change in velocity
σ_{ij} elements of S
k time step
t_0 initial time
$\boldsymbol{u}_0$ the initial velocity for a track minus the mean velocity
$\boldsymbol{x}_0 = (y_0, z_0)$ the initial position for a track
Δt the time difference between two time steps in an observed track
E_{eb} the event of being within A_{eb} at t_{eb}
A_{eb} the area defining the echo beam in the 2D plane
t_{eb} the time when the vessel-mounted echosounder is passing the 2D plane
E_{tr} the event of being within A_{tr} at t_{tr}
A_{tr} the area defining the trawl availability window in the 2D plane
t_{tr} the time when the trawl doors is passing the 2D plane
N number of simulated individuals for each run
N_{eb} the number of simulated individuals satisfying E_{eb}
N_{tr} the number of simulated individuals satifying E_{tr}
$N_{\text{eb},A}$ echo beam encounters
$N_{\text{tr},A}$ trawl encounters
$N^0_{\text{tr},A}$ nondisturbed trawl encounters
A the 2D model domain
$P\{\text{event}\}$ the probability of an event to occur
$\widehat{\ }$ hat symbol; indicates that the variable is estimated from data
$\Delta t_{\max}$ the maximum Δt used in the curve fitting
$\boldsymbol{y}_{jk} = (y_{1jk}, y_{2jk})$ the position of track j at time t_k
A_k the set of tracks j present at time t_k
Δ lag in terms of time steps (integer)
s_i integrated mean movement
h the bandwidth parameter for the kernel smoothing function
F_i estimate of $E\{[\boldsymbol{X}'_i(t_{k+\Delta}) - \boldsymbol{X}'_i(t_k)]^2 | X_2 = z\}$
z_{d} upper bound of dead zone
z_{h} head line height
y_b trawl door spread
$k_{h3}k_{v3}$ parameters in the Dickson (1993*a*) model
h_{d} dead zone behaviour
p_{d} proportion of fish originally in dead zone
t_{tow} tow time
ρ_a horizontal area density
$f(z_0)$, $g(z_0)$ relative vertical profiles

Appendix A. Estimating the model parameters based on tracking data

The data for each track is of the form $\boldsymbol{y}_{jk} = (y_{1jk}, y_{2jk})$, where y_1 is the track position in the horizontal coordinate (y), y_2 is the coordinate in the vertical direction (z), j denotes track number, and k denotes the position at time step k along the track, corresponding to the time step t_k. Recall that we used $\boldsymbol{X}_{t_k} = (Y_{t_k}, Z_{t_k}) = [X_1(t_k), X_2(t_k)]$ for the vector process representing the fish track including the drift term $\boldsymbol{m}$, and $\boldsymbol{X}'_{t_k} = (Y'_{t_k}, Z'_{t_k}) = [X'_1(t_k), X'_1(t_k)]$ for the process excluding the drift term. Each track is, of course, not present in the coordinate system for all times t_k. It is therefore useful to define A_k, the set of tracks j present in ping k.

First we estimate the drift term $\boldsymbol{m}(z, t) = (m_1, m_2)$ of eq. 1 for each t_k and depth z. For time step t_k and depth z, we start by introducing for $i = 1, 2$:

$$\text{(A1)} \qquad \widehat{s}_i(t_k, z, \Delta) = \int_{t_k}^{t_{k+\Delta}} m_i(z, s)\, \mathrm{d}s = \frac{\sum_{j \in \{A_k \cup A_{k+\Delta}\}} \{(y_{ij,k+\Delta} - y_{ijk}) K_h(z - y_{2jk})\}}{\sum_{j \in \{A_k \cup A_{k+\Delta}\}} K_h(z - y_{2jk})}$$

as an estimate for the integrated mean movement in each dimension. Here K is a kernel smoothing function centered on z, Δ represents the lag in terms of time steps (it is an integer, not to be confused with Δt), and A_k and $A_{k+\Delta}$ are the set of tracks present in time steps t_k and $t_{k+\Delta}$. We have used a Gaussian kernel function $K(s) = \frac{1}{\sqrt{2\pi}} \exp(-\frac{1}{2} s^2)$ and $K_h(s) = h^{-1}K(s/h)$, where h is a bandwidth parameter that has been set to 35 m. Equation A1 then represents an estimate of $E\{X_i(t_{k+\Delta}) - X_i(t_k) | X_2 = z\}$, which is an advection term for the mean movement of the individuals. The resulting estimate of the mean motion $\widehat{m}_i(z, t) = \widehat{s}_i(t_k, z, 1)/(t_{k+1} - t_k)$, as presented in eq. 1, is obtained by setting $\Delta = 1$ and dividing eq. A1 by the time difference $t_{k+1} - t_k$.

The next step is to estimate the diffusion parameters σ_{ii} and β_{ii}. As a first step, we estimate nonparametrically the left-hand side $E\{[X'_i(t_{k+\Delta}) - X'_i(t_k)]^2 | X_2 = z\}$ of eq. 5, representing time t_k and depth z, by

$$\text{(A2)} \qquad F_{ii}(t_k, z, \Delta) = \frac{\sum_{j \in \{A_k \cup A_{k+\Delta}\}} \{[y_{ij,k+\Delta} - y_{ijk} - \widehat{s}_i(t_k, z, \Delta)]^2 K_h(z - y_{2jk})\}}{\sum_{j \in \{A_k \cup A_{k+\Delta}\}} K_h(z - y_{2jk})}$$

for $i = 1,2$, representing the athwartship and depth component with the estimated mean motion subtracted. The parameters F_{ii} are dependent on the time step lag Δ, and the form of this curve is the basis on which the models are chosen (see Fig. A1). In the figure, the curves are presented by dividing F_{11} and F_{22} by $(t_{k+\Delta} - t_k)$. The curve seems to reach an asymptotic value for larger time lags, which is consistent with eq. 17 when divided by Δt. For a Wiener process, the variance is proportional to Δt. This would be a horizontal line in this plot and is not in agreement with our data.

We also estimated the covariance term $E\{[X'_1(t_{k+\Delta}) - X'_1(t_k)][X'_2(t_{k+\Delta}) - X'_2(t_k)] | X_2 = z\}$ of the residual process $\boldsymbol{X}'_t$ by

$$\text{(A3)} \qquad F_{12}(t_k, z, \Delta) = \frac{\sum_{j \in \{A_k \cup A_{k+\Delta}\}} \left\{ \left[\prod_{i \in \{1,2\}} \left(y_{ij,k+\Delta} - y_{ijk} - \widehat{s}_i(t_k, z, \Delta) \right) \right] K_h(z - y_{2jk}) \right\}}{\sum_{j \in \{A_k \cup A_{k+\Delta}\}} K_h(z - y_{2jk})}$$

where Π denotes product between the following terms. Based on the small magnitude of the estimated F_{12}, the terms β_{12} and σ_{12} in eqs. 3 and 4, respectively, were neglected.

Outliers are removed before implementing the operations of eqs. A2 and A3. A difference $D = y_{ij,k+\Delta} - y_{ijk}$ is defined as an outlier if $D < q_1 - 1.5\,\mathrm{IQR}$ or $D > q_3 + 1.5\,\mathrm{IQR}$, where q_1 and q_3 are the first and third quartiles, respectively, and $\mathrm{IQR} = q_3 - q_1$ is the interquartile range in the distribution of D.

To estimate the OU parameters σ_{ii} and β_{ii} for a given time t_k and depth z, the estimates of F_{ii} (eq. A2) are fitted to the functional form of the variance term of the OU process (eq. 5) by minimizing

$$\text{(A4)} \qquad \min_{\{\sigma_{ii}, \beta_{ii}\}} \left\{ \sum_{\Delta} \left[\frac{\sigma_{ii}^2}{\beta_{ii}^3} [\beta_{ii}(t_{k+\Delta} - t_k) - 1 + \exp[-\beta_{ii}(t_{k+\Delta} - t_k)]] - F_{ii}(t_k, z, \Delta) \right]^2 w_i(t_k, \Delta) \right\}$$

for different t_k and z. Note that the parameters σ_{ii} and β_{ii} depend on time and depth, but are assumed constant for each t_k and z. Here $i = 1,2$, F_{ii} is taken from eq. A2, and $w_i(t_k, \Delta) = N/\mathrm{SD}_j\{[y_{ij,k+\Delta} - y_{ijk} - \widehat{s}(t_k, z, \Delta)]^2\}$ is a weight function, with N being the number of tracks present in both bins A_k and $A_{k+\Delta}$, and with SD_j is the standard deviation taken as j varies for a fixed i, Δ, and t_k. The parameter estimates are found by minimizing eq. A4 using the Nelder–Mead simplex (direct search) method (Lagarias et al. 1998) implemented in the Matlab (c) function fminsearch. Examples of the curve fitting are given in Fig. A1. Note that the asymptotic value of the fitted curve is equivalent to the effective diffusion described in the Materials and methods section.

Fig. A1. An example of fitting curves for (*a*) $F_{11}/\Delta t$ and (*b*) $F_{22}/\Delta t$, where $\Delta t = t_{k+\Delta} - t_k$. The example is taken for $t = -1$ s and $d = -260$ m, and the corresponding parameter estimates are $\widehat{\sigma}_{11} = 0.061$ and $\widehat{\beta}_{11} = 0.1$ for panel (*a*) and $\widehat{\sigma}_{22} = 0.062$ and $\widehat{\beta}_{22} = -0.018$ for panel (*b*).

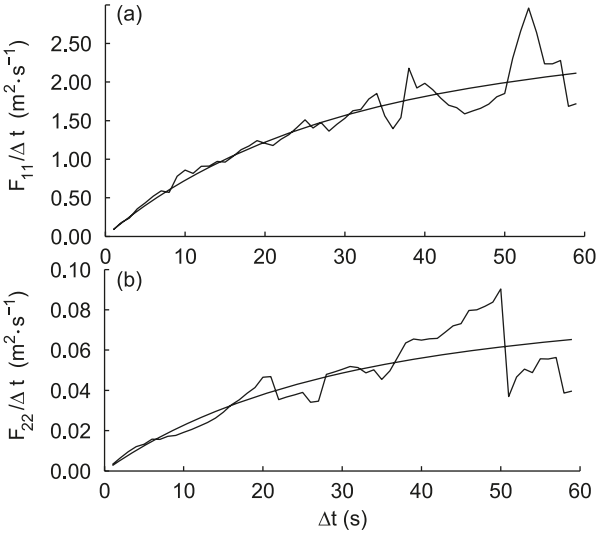

The resulting parameters as a function of depth and time are further processed by first removing outliers (same definition as above). If the parameter estimation by fminsearch fails for a time–depth pair, linear interpolation in time is used as an estimatefor that pair. After the estimation, a running mean filter of ±3 min is applied to further smooth the data in the time dimension.

The result of these procedures are the parameters $\boldsymbol{m}$, σ_{ii}, and β_{ii} resolved in z (depth) and t_k (time before or after vessel–buoy passing), and the parameters are estimated for all the different estimators or degrees of smoothing described in the Materials and methods section.

Reference

Lagarias, J., Reeds, J.A., Wright, M.H., and Wright, P.E. 1998. Convergence properties of the Nelder–Mead simplex method in low dimensions. SIAM J. Optim. **9**(1): 112–147. doi:10.1137/S1052623496303470.